The Journal of Physical Chemistry

VOLUME 92, NUMBER 20 OCTOBER 6, 1988

LETTERS

Spectroscopic Mapping of the OH–Ar van der Waals Potential

Mary T. Berry, Mitchell R. Brustein, Joseph R. Adamo, and Marsha I. Lester*,†

Department of Chemistry, University of Pennsylvania, Philadelphia, Pennsylvania 19104-6323
(Received: June 8, 1988)

Fluorescence excitation spectra of OH–Ar van der Waals (vdW) complexes are observed in the spectral region about the OH $A^2\Sigma^+(v'=0)$–$X^2\Pi_{3/2}(v''=0)$ transition. A vibrational progression, consisting of seven elements with similar rotational structure, is assigned to an OH–Ar vdW stretching mode in the excited state. The last member of the progression provides a lower limit for the OH–Ar binding energy $D_0(v'=0)$ of 521 cm^{-1}. An estimate for the ground-state binding energy $D_0(v''=0)$ of ≥ 24 cm^{-1} is obtained from the spectral shift of the vdW vibrational feature to free OH. A comparison is made with an analogous low-frequency vibrational mode previously reported upon electronic excitation of OH in an Ar matrix.

Introduction

Spectroscopic experiments on weakly bound atomic or molecular aggregates, known as van der Waals (vdW) complexes, provide a unique way to probe the intermolecular potential between the molecules. The geometry of the complex,[1-3] often derived from rotationally resolved spectra, reflects the balance of forces at the zero-point level of the potential well. In principle, the attractive well region of the intermolecular potential can be characterized through spectroscopic interrogation of vibrationally excited vdW motions. The vdW binding energy can be determined by accessing a succession of vdW vibrational levels and extrapolating to the dissociation limit.[4] Complementary information on the repulsive, short-range part of the potential is usually obtained from scattering experiments.

In this Letter, we report the direct spectroscopic mapping of the intermolecular potential between Ar and hydroxyl radicals in the $A^2\Sigma^+$ state along the minimum-energy approach. This provides a new basis for understanding the collision dynamics proceeding on the full anisotropic potential energy surface. Since hydroxyl radicals are sufficiently small to be theoretically tractable, the form of the interaction potential of OH with various collision partners is of special importance. The hydroxyl radical is also of particular interest because it is an open-shell system with spin–orbit interactions in the ground state.

Collisional studies of hydroxyl radicals in the $A^2\Sigma^+$ state with a variety of partners have shown that attractive, long-range forces dominate the relaxation dynamics.[5] The high efficiency for inelastic energy-transfer processes has been correlated with the formation of a transitory "collision complex" due to anisotropic attractive forces in the entrance channel of the potential energy surface.[6] Recently, ab initio potential surfaces have been constructed to investigate inelastic scattering of He and CO with OH in the $X^2\Pi_i$ and $A^2\Sigma^+$ states.[7] The results presented here provide

†Alfred P. Sloan Research Fellow and Camille and Henry Dreyfus Foundation Teacher–Scholar.

(1) Miller, R. E. *J. Phys. Chem.* **1986**, *90*, 3301.
(2) Celli, F. G.; Janda, K. C. *Chem. Rev.* **1986**, *86*, 507. Janda, K. C. *Adv. Chem. Phys.* **1985**, *60*, 201.
(3) Levy, D. H. *Adv. Chem. Phys.* **1981**, *47*, 323.
(4) Drobits, J. C.; Lester, M. I. *J. Chem. Phys.* **1987**, *86*, 1662.
(5) Copeland, R. A.; Crosley, D. R. *J. Chem. Phys.* **1986**, *84*, 3099. Jeffries, J. B.; Copeland, R. A.; Crosley, D. R. *J. Chem. Phys.* **1986**, *85*, 1898.
(6) Lengel, R. K.; Crosley, D. R. *J. Chem. Phys.* **1978**, *68*, 5309. Fairchild, P. W.; Smith, G. P.; Crosley, D. R. *J. Chem. Phys.* **1983**, *79*, 1795. Copeland, R. A.; Dyer, M. J.; Crosley, D. R. *J. Chem. Phys.* **1985**, *82*, 4022.

0022-3654/88/2092-5551$01.50/0

the first experimental data on the actual form of the Ar + OH $A^2\Sigma^+$ potential in the gas phase and directly yield the depth of the attractive well in the ground and excited states.

Experimental Section

Ultracold hydroxyl radicals and hydroxyl–argon vdW complexes are produced in a supersonic expansion of ultraviolet photolyzed nitric acid in pure Ar carrier gas (60 psi). The HNO_3/Ar gas mixture is expanded into the vacuum apparatus through a quartz capillary tube (1-cm length, 0.5-mm bore) mounted to the faceplate of a pulsed valve. The HNO_3 is photolyzed in the capillary[8] at the peak of the gas pulse with an ArF excimer laser at 193 nm. The excimer laser is focused onto the capillary, irradiating a 2-mm length near the end of the capillary and filling the bore.

The OH radicals and OH–Ar complexes are probed approximately 1.5 cm downstream of the capillary nozzle exit. Tunable laser radiation in the vicinity of the OH $A^2\Sigma^+(v'=0)$–$X^2\Pi_{3/2}$ $(v''=0)$ transition at 307–313 nm (~0.5 mJ/pulse) is generated by frequency doubling the output of an excimer pumped dye laser (Kiton Red) in KDP with a home-built autotracking device. The OH radicals and OH–Ar vdW complexes can be detected over a 5-μs-fwhm range within the nearly 1-ms gas pulse exiting from the capillary nozzle source.

Laser-induced fluorescence is detected normal to both the probe laser and nozzle beam axes. Only the central core of the expansion is imaged in order to reduce Doppler broadening resulting from the angular divergence of the jet to less than the laser bandwidth (0.15 cm^{-1}). A 0.25-m monochromator acts as a broad-band filter, passing emission over an approximately 3-nm bandwidth about the excitation wavelength. In these experiments, fluorescence must be detected in the presence of intense background signals due to direct scatter at 193 nm and a spectrally broad, long-lived emission resulting from ArF irradiation of the quartz tubing. The background signals are reduced in intensity with filters that block 193-nm (WG-295) and visible (UG-5) light. In addition, the photomultiplier tube (EMI 9813Q) is gated "off" during the photolysis pulse.

Results

Fluorescence excitation spectra of OH radicals produced upon ultraviolet photolysis of the HNO_3/Ar gas mixture have been recorded in the region of the OH $A(v'=0)$–$X(v''=0)$ transition. Under the supersonic expansion conditions described above, only the three OH rotational transitions (with associated satellite structure) originating from $N''=1$, $J''={}^3/_2$ are observed. The sparse number of lines detected demonstrates that the ground-state OH population has been collapsed into a single rotational level.

Under identical expansion conditions, a series of new features appear in the vicinity of the well-characterized OH $A(v'=0)$–$X(v''=0)$ transition. To date, 10 new features have been identified, each containing extensive rotational structure. These new features are attributed to the OH–Ar vdW molecule. The features arise from rovibronic excitation into the OH–Ar vdW potential which correlates with $OH(A^2\Sigma^+(v'=0)) + Ar(^1S_0)$.

The lowest energy feature, occurring at 31 944.1 cm^{-1}, is shifted 496.5 cm^{-1} toward lower energy of the OH $P_1(1)$ transition. The spectroscopic shift is a measure of the relative binding energies of $Ar(^1S_0)$ to OH in its ground $X(v''=0)$ and excited $A(v'=0)$ states. The shift of the lowest energy vdW feature relative to the OH $P_1(1)$ transition indicates that the complex is significantly more tightly bound in the excited state.

Seven of the features exhibit similar rotational envelopes. The rotational structure consists of a sharp bandhead at the low-wavenumber extreme, a large central peak, and a series of more widely spaced lines extending to the high-wavenumber side of the band. A low-resolution scan over the feature centered at 32 371.3 cm^{-1} is shown in Figure 1. The positions of these seven features, measured at the central peak, are given in Table I.

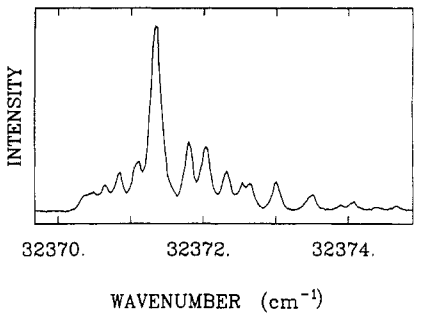

Figure 1. Fluorescence excitation spectrum illustrating the rotational envelope of one of the seven OH–Ar features which form a vibrational progression in the vicinity of the OH $A(v'=0)$–$X(v''=0)$ transition. The feature arises from rovibronic excitation into the OH–Ar van der Waals potential correlating with $OH(A^2\Sigma^+(v'=0)) + Ar(^1S_0)$.

TABLE I: Positions (cm^{-1}) and Spacings between Spectral Features, ΔG (cm^{-1}), Assigned to Vibrational Progression in OH–Ar Stretching Mode

van der Waals complex[a]			matrix[b]	
position	ΔG	v[c]	position	ΔG
		(0)	31 547	
31 944.1		(1)	31 715	168
32 078.2	134.1	(2)	31 868	153
32 193.8	115.6	(3)	31 991	123
32 291.3	97.5	(4)	32 083	92
32 371.3	80.0	(5)	32 155	72
32 432.9	61.6	(6)		
32 464.9	32.0	(7)		

[a] This work. [b] Reference 9. [c] Vibrational quantum number assignments taken from matrix data (ref 9).

We assign the features listed in Table I to a vibrational progression in the OH–Ar vdW stretching mode. The spacing between successive bands, ΔG, decreases as the transition energy increases. The anharmonicity in the vibrational motion is nearly constant over the entire progression, as indicated by the difference in ΔG values. The relative intensities of the bands listed in Table I generally follow a smooth Franck–Condon profile, peaking at the 32 291.3- and 32 371.3-cm^{-1} features and falling off toward higher and lower energy, except the highest energy feature which exhibits a larger intensity than that of the preceding element in the progression.

The three features which are not included in the assigned vibrational progression are found at 32 534, 32 502, and 32 402 cm^{-1}. These features show no bandhead and exhibit rotational spacings that differ from each other and from the seven elements of the progression listed in Table I. These features may be due to another vdW vibrational mode (e.g., bend) or to higher order clusters (e.g., $OH–Ar_2$). The latter seems likely for the structure centered at 32 502 cm^{-1}, which shows more tightly spaced rotational lines.

Discussion

A Birge–Sponer analysis of the OH–Ar van der Waals progression has been performed to estimate the binding energy of Ar to OH in the $A(v'=0)$ state, as well as the vibrational constants for the OH–Ar vdW stretch. The spacing between successive bands in the progression (ΔG) is plotted as a function of the vdW vibrational quantum number (v_{vdW}) in Figure 2. The choice for vibrational quantum number assignments is discussed below. The linear fit in Figure 2 indicates that a simple anharmonic oscillator well characterizes the vibrational motion in the spectroscopically accessed portion of the potential well.

The anharmonicity in the vibrational progression, derived from a least-squares fit of the slope of the Birge–Sponer plot, is $\omega_e x_e = 9$ cm^{-1}. Values for the fundamental frequency, ω_e, and the vdW bond dissociation energy, $D_0(v'=0)$, depend on the vdW vibrational quantum number assignment. If the lowest observed vibrational

(7) Farantos, S. C.; Vegiri, A. *J. Phys. Chem.* **1988**, *92*, 2719. Vergiri, A.; Farantos, S. C. *J. Phys. Chem.* **1988**, *92*, 2723. Vegiri, A.; Farantos, S. C.; Papagiannakopoulos, P.; Fotakis, C. *J. Phys. Chem.*, to be published.
(8) Andresen, P.; Hausler, D.; Lulf, H. W. *J. Chem. Phys.* **1984**, *81*, 571.

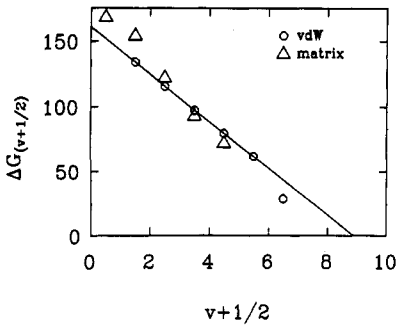

Figure 2. Birge–Sponer plot relating the spacings between successive vibronic transitions (ΔG) to the vibrational quantum number (v) for the OH–Ar stretching mode in the van der Waals complex (this work) and in matrix isolation (ref 9).

level is taken to be the vibrational origin, ω_e is evaluated at 152 cm^{-1}. A linear Birge–Sponer extrapolation yields the vdW binding energy, $D_0(v'=0)$ = 565 cm^{-1}.

Goodman and Brus[9] have identified a similar low-frequency vibrational mode upon electronic excitation of hydroxyl radicals imbedded in a solid argon matrix. An anharmonic vibrational progression consisting of 6–7 members was observed associated with each of the OH $A(v'=0–2)$–$X(v''=0)$ transitions. Analogous vibronic structure was detected for OH isolated in a dilute mixture of Ar in a Ne host matrix, although excitation features were more extensively broadened. The vibrational progression in the matrix data was attributed to an OH–Ar stretch in an excited state, correlating with $OH(A^2\Sigma^+)$ + Ar. The vibrational motion was associated with OH interacting with a single Ar nearest neighbor, which was unaffected by the addition of other Ar neighbors.

The transitions reported by Goodman and Brus for the OH–Ar progression in an Ar matrix are reproduced in Table I. Although the absolute frequencies of the OH–Ar transitions differ for the van der Waals complex and the matrix, the spacings between successive vibronic transitions are remarkably similar. Comparison of the matrix and gas-phase data indicates that the vibrational progression observed in the matrix may begin one vibrational level lower than that detected for the vdW complex. The OH–Ar vdW progression also extends two vibrational levels beyond that observed in the matrix. We adopt the vibrational quantum number assignments used for analysis of the matrix data, so that the lowest energy feature in the vdW spectrum is assigned as v_{vdW} = 1. A search was made in the vdW spectrum for an origin feature corresponding to that reported in the matrix but was not observed at the present detection sensitivity.

The Birge–Sponer plot shown in Figure 2 illustrates the vibrational progressions observed for the OH–Ar vdW complex and OH in an Ar matrix, using the latter vibrational quantum number assignments. This numbering scheme yields a fundamental vibrational frequency ω_e = 170 cm^{-1} and binding energy $D_0(v'=0)$ of 718 cm^{-1} for the OH–Ar vdW complex. The calculation of D_0 relies on the validity of a linear extrapolation procedure. Birge–Sponer plots often exhibit significant curvature near the dissociation limit, due to the increasing importance of higher order anharmonicity terms in the potential. The Birge–Sponer plot may deviate from linear near the OH–Ar dissociation limit, as suggested by the negative offset of the last point in Figure 2.

The binding energy of Ar to OH in the $X(v''=0)$ state can be evaluated from the spectroscopic shift of the assigned vdW vibrational origin from the free OH $P_1(1)$ transition and the binding energy of OH–Ar in the excited state. Since both $D_0(v'=0)$ and the spectroscopic shift change in the same manner with assignment of the vdW vibrational origin v_{vdW} = 0, any numbering choice will lead to

$$D_0(v''=0) = D_0(v'=0) - \text{shift} = 69\ cm^{-1}$$

This value for $D_0(v''=0)$ depends on the accuracy of the Birge–Sponer extrapolation used to obtain $D_0(v'=0)$.

A lower bound for $D_0(v'=0)$ can be set by assuming that the last element observed in the vdW progression lies just below the OH–Ar dissociation limit. This gives $D_0(v'=0) \geq 521\ cm^{-1}$ and $D_0(v''=0) \geq 24\ cm^{-1}$.

Goodman and Brus[9] have suggested that matrix-isolated OH–Ar has a linear structure in both the ground (X) and excited (A) states. If the OH–Ar complex exists as a linear molecule in the gas phase, the rotational structure observed in Figure 1 would correspond to a P branch with a bandhead, a central Q branch whose high-J lines would extend into the R branch, and an R branch. The increased spacing between R-branch lines with increasing J would then reflect the change in moments of inertia between the ground and excited states. The appearance of a bandhead on the low-frequency side of the rotational contour indicates that the OH–Ar equilibrium bond distance decreases upon electronic excitation. The extensive vibrational progression observed in the OH–Ar stretching mode implies a significant change in the vdW bond length. This is consistent with the matrix data, which yielded a smaller bond length (Δr_e = 1.15 ± 0.1 Å) for the excited state of OH–Ar through a Franck–Condon analysis.[9]

A preliminary rotational analysis of four spectral features in the OH–Ar vdW stretching progression (v_{vdW} = 2–5) yields a vdW bond length (OH center-of-mass to Ar distance) of 2.8 Å at the equilibrium position (r_e) of the excited-state OH–Ar potential and an average vdW bond length of 3.5 Å at the zero-point level of the ground state. A detailed description of the rotational analysis performed on the OH–Ar vdW molecule will be presented elsewhere.[10]

In this experiment we have demonstrated that OH–Ar complexes can be prepared with vibrational excitation directly in the vdW bond dissociation coordinate via the vdW stretch reported here. This opens fascinating new possibilities for future studies on the vibrational predissociation dynamics of OH–Ar complexes. Now, in addition to evaluating the rate of vibrational predissociation and product-state distribution following excitation of the OH vibrational motion, analogous to experiments performed in this laboratory on ICl–rare gas complexes,[11] the dynamics can be explored upon vibrational excitation of the OH–Ar vdW bond.

Acknowledgment. The authors thank Paul Arias and John Gardner for their valuable contributions to an early phase of this work. This research was supported by the Division of Chemical Sciences, Office of Basic Energy Sciences, of the Department of Energy. M.I.L. gratefully acknowledges the Natural Science Association at the University of Pennsylvania for a Young Faculty Award.

(9) Goodman, J.; Brus, L. E. *J. Chem. Phys.* **1977**, *67*, 4858.
(10) Berry, M. T.; Brustein, M. R.; Lester, M. I. *Chem. Phys. Lett.*, to be published.
(11) Drobits, J. C.; Skene, J. M.; Lester, M. I. *J. Chem. Phys.* **1986**, *84*, 2896. Skene, J. M.; Drobits, J. C.; Lester, M. I. *J. Chem. Phys.* **1986**, *85*, 2329. Drobits, J. C.; Lester, M. I. *J. Chem. Phys.* **1988**, *88*, 120.